Amphoteric Surfactant-Chelating Agent Interactions: Impact on Bulk and Surface Properties

Journal of Colloid and Interface Science 694 (2025) 137606

Contents lists available at ScienceDirect

Journal of Colloid And Interface Science

journal homepage: www.elsevier.com/locate/jcis

Amphoteric Surfactant-Chelating Agent Interactions: Impact on Bulk and Surface Properties

Josmary Velásquez [a,b], Sarah Lundgren [a], Lars Evenäs [b], Romain Bordes [b,*]

[a] Nouryon Surface Chemistry AB, Stenungsund, Sweden
[b] Department of Chemistry and Chemical Engineering, Chalmers University of Technology, Gothenburg, Sweden

GRAPHICAL ABSTRACT

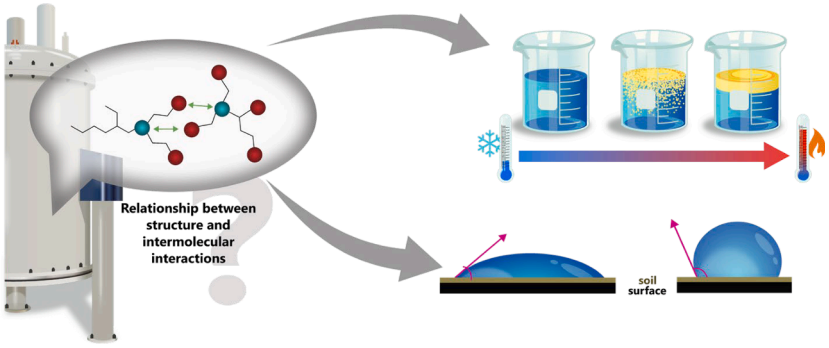

ARTICLE INFO

Keywords:
Chelating Agents
Surfactants
NMR
Formulation
Wetting

ABSTRACT

Hypothesis: Recent findings indicate that there are interactions between amphoteric surfactants and chelating agents in solution, which influence the capacity of the system to solubilize non-water-soluble nonionic ethoxylated surfactants. We hypothesize that these interactions are primarily driven by the chemical affinity between the head groups of the amphoteric surfactant and the chelating agent. By modulating the strength of this interaction, it may be possible to control the surface properties of the mixed system containing non-water-soluble nonionic ethoxylated surfactants.

Experiments: To investigate the relationship between chemical structure and the previously reported interactions, we employed a set of amine-containing surfactants and polycarboxylic acid-type chelating agents. The interactions were monitored using NMR spectroscopy, specifically through ^{13}C chemical shift and line shape analysis. The impact of these interactions on surface properties was assessed by measuring surface tension and contact angle on hydrophobic surfaces.

Findings: The occurrence of interactions between surfactants and chelating agents depends heavily on their structure and is found stronger when both surfactants and chelating agents bear both positive and negative charges. Since the interactions take place in solution, it increases system solubilization power, yet the surface properties of the complexes are not affected by the interactions. However, when a poorly soluble nonionic surfactant is introduced, improved wetting properties are observed.

* Corresponding author.
E-mail address: bordes@chalmers.se (R. Bordes).

https://doi.org/10.1016/j.jcis.2025.137606
Received 30 January 2025; Received in revised form 25 March 2025; Accepted 14 April 2025
Available online 15 April 2025

1. Introduction

Aqueous surfactant systems are widely used in industrial applications, often relying on untreated water sources that contain metal ions. The present metal ions reduce solubility of the surfactant and can form insoluble precipitates, which disrupt the performance of the cleaning system. To mitigate these effects, chelating agents are commonly used to complex metal ions stoichiometrically, improving the solubility and transport of metal ions in solution [1–3]. This property helps preventing crystal growth and inhibits catalytic reactions that could be detrimental to the product. Chelating agents are also valuable in environmental applications and medical treatments for removing toxic metals, as well as in agriculture, where they enhance the availability and transport of nutrient metals.

Despite their importance and wide applicability, little information is available on the effect of chelating agents on self-assembly behavior and surface properties of surfactants. Existing literature falls mainly into two categories: (i) studies focused on traditional chelating agents like ethylenediamine tetraacetic acid (EDTA) [4–6], which has limited biodegradability and is now being replaced by more eco-friendly alternatives like methylglycinediacetic acid (MGDA) and L-glutamic acid N,*N*-diacetic acid (GLDA) [7,8]; and (ii) research with an emphasis on applications, often lacking in-depth exploration of the chemical mechanisms driving these processes [9–11].

Chelating agents of the aminopolycarboxylate type, such as EDTA, have been studied by Zhao *et al.*, who examined the effects of EDTA on gemini cationic surfactants. Their findings showed that EDTA induces the formation of oligomeric surfactant analogues that self-assemble at concentrations below the CMC of the pure surfactant, a phenomenon attributed to electrostatic binding between the carboxylate groups of EDTA and the ammonium moiety in the surfactant [4]. Another study by Soontravanich *et al.* explored the synergistic behavior in the solubility of soap scum at high pH when combining amine oxide-based surfactants with EDTA, achieving solubility levels approximately three times higher than in chelate-free systems. They attributed this to mixed micelle formation between stearate anions and the surfactant, facilitated by EDTA and the chelated Ca^{2+} ions [5].

Yunusov *et al.*[6] explored the molecular behavior of surfactant-EDTA systems using molecular simulations. Their findings indicated that, according to density profiles, EDTA accumulates near the water-octane interface, contributing to a thicker interfacial layer. This effect was also observed in systems containing surfactants and chelating agents. The addition of EDTA disrupts hydrogen bonding, both between water molecules and between water and surfactant molecules, suggesting that EDTA acts as a salting-out agent. Moreover, a decrease in the hydration of surfactants was observed, accompanied by an enhanced monolayer packing due to electrostatic repulsion, as indicated by the radial distribution function calculations. Additionally, the interaction between the chelating agent and sodium dodecyl sulfate was found to promote surfactant adsorption at the water-hydrocarbon interface, which contributed to a reduction in interfacial tension.

Literature on MGDA and GLDA predominantly focuses on practical applications, such as enhanced oil recovery in oil fields [9,10] and cloud point extraction for water treatment processes [11]. These studies generally investigate performance metrics such as recovery and surface tension variations as experimental variables are adjusted. To the best of

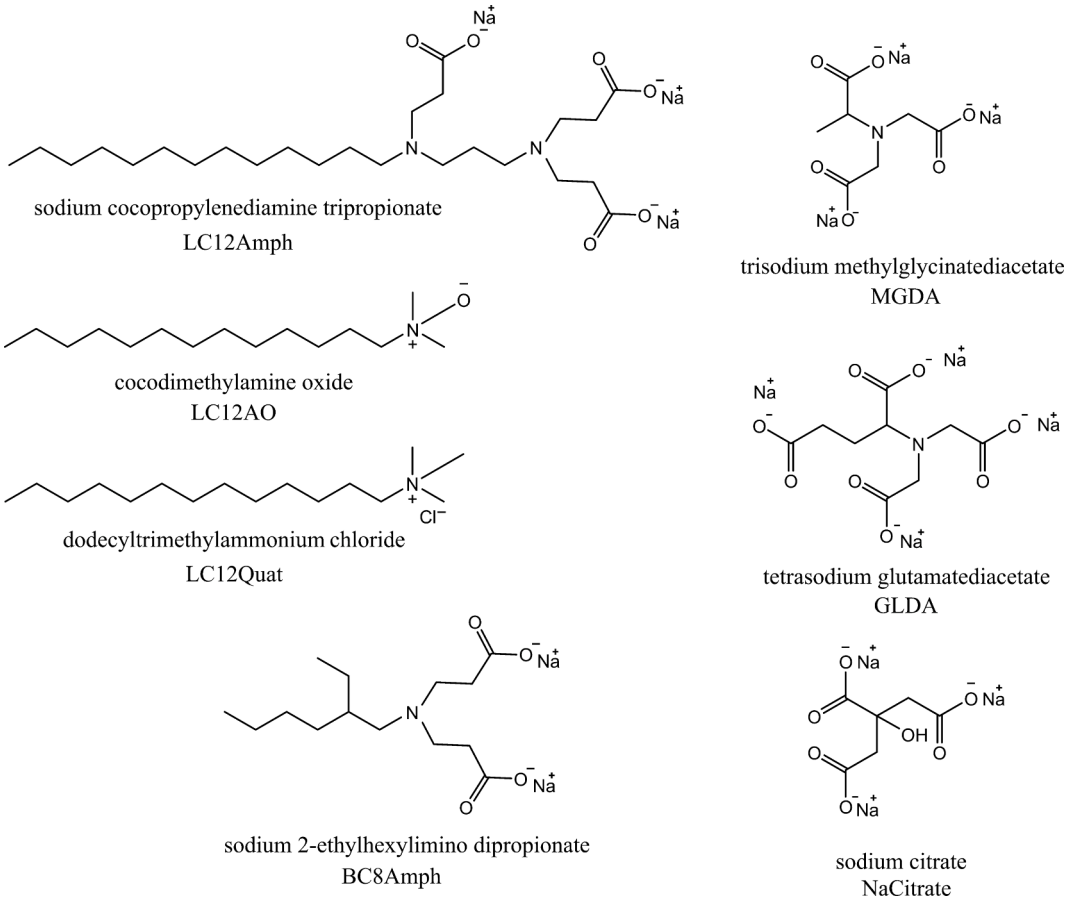

Fig. 1. Chemical structures of the chelating agents and surfactants evaluated in this study. Surfactants are sodium cocopropylenediamine tripropionate (LC12Amph), cocodimethylamine oxide (LC12AO), dodecyltrimethylammonium chloride (LC12Quat), and sodium 2-ethylhexylimino dipropionate (BC8Amph). Chelating agents are trisodium methylglycinatediacetate (MGDA), tetrasodium glutamatediacetate (GLDA), and sodium citrate (NaCitrate). The abbreviated names used throughout the article are also indicated for clarity.

our knowledge, no existing literature provides molecular-level analyses of systems combining these chelating agents with surfactants.

To address this research gap, we have previously reported on the effect of GLDA on aggregation behavior of an amphoteric surfactant using ^{13}C NMR chemical shift and line shape analysis, and ^{1}H diffusometry [12]. Our findings revealed an interaction between the surfactant headgroup and the chelating agent, characterized by several key observations: (i) there is as an equilibrium between interacting and non-interacting species; (ii) GLDA interacts with both unimeric surfactants and with micellized surfactants; (iii) the interaction preferentially occurs at the carbonyl groups closest to the nitrogen atom of GLDA; and (iv) the micellar size decreases in the presence of GLDA.

As a result of this interaction, a complex-like surfactant is formed, characterized by an enlarged head group. In systems containing a water-insoluble nonionic surfactant, the reduced micellar size leads to lower viscosity and increased cloud point; furthermore it allows for the solubilization of larger quantities of the nonionic surfactant. Our preceding work focused on a single surfactant-chelating agent pair; here, we aim to expand the study to a broader range of surfactant-chelating agent systems.

Building on our previous findings, this study extends the investigation to examine structure–property relationships within a broader matrix of amine-containing surfactants and polycarboxylic acid-type chelating agents. The chemical structures and our corresponding abbreviations for these compounds are provided in Fig. 1. Following our experimental methodology [12], we focused on the low-field region of the ^{13}C NMR spectra, where signals from the carbonyl carbons reveal the most significant insights into the interacting species.

The selection of specific chelating agents and surfactants was guided by both their commercial relevance and subtle structural variations to better understand the role of particular atoms in these interactions. For example, sodium citrate serves as a structural analog to MGDA but lacks a nitrogen atom in its core, providing a useful basis for comparison. This work investigates how small modifications in the structure of chelating agents influence their interaction with amphoteric surfactants, as well as how structural changes in surfactants affect their interaction with chelating agents. Additionally, we assess the impact of these interactions on bulk properties, such as cloud point, and on surface properties, including surface tension and contact angle.

2. Experimental methods

2.1. Materials

The chemicals used in this study included ethoxylated decyl alcohol with four ethoxylated groups (C10E4, pH = 6.5), sodium 2-ethylhexylimino dipropionate (BC8Amph, pH = 9, pKa = 10.2), sodium cocopropylenediamine tripropionate (LC12Amph, pH = 6.5, pKa = 8.4, 9.9), cocodimethylamine oxide (LC12AO, pH = 7), tetrasodium glutamatediacetate (GLDA, pH = 11.4, pKa = 9.5), and trisodium methylglycinatediacetate (MGDA, pH = 11, pKa = 9.5), all supplied by Nouryon. The reported pH values correspond to 1 % w/w solutions measured using a Mettler Toledo FiveGo F2 IP67 pH meter, while pKa values were estimated using ChemDraw. Sodium citrate (NaCitrate, ≥99 % purity) and dodecyltrimethylammonium chloride (LC12Quat, ≥98 % purity) were purchased from Sigma Aldrich. All chemicals were used as received.

The surfactants are named according to the following convention: the first letter indicates the structure of the lipophilic chain, with “L” for linear and “B” for branched, followed by a number that denotes the length of the hydrocarbon chain. The remainder of the abbreviation describes the nature of the head group of the surfactant.

Milli-Q water, with a resistivity of ≥ 18.2 MΩ·cm at 25 °C and total organic carbon content below 400 ppb, was used throughout the study.

2.2. NMR spectroscopy

The NMR samples were prepared with a constant concentration of chelating agent (0.24 M) while varying the surfactant concentration. To achieve this, a stock solution containing both surfactant and chelating agent was incrementally diluted with a separate stock solution containing only the chelating agent. The pH of the prepared samples was not adjusted but measured, with values ranging between 9 and 10.

All NMR measurements were conducted on a 400 MHz Varian VNMRS spectrometer, maintained at 25 ± 0.1 °C. Each 5 mm NMR tube contained a sealed glass capillary with deuterated methanol (99.6 % purity, Fisher Scientific), used as both the ^{2}H locking solvent and ^{13}C chemical shift reference, with the MeOD signal calibrated to 49 ppm. The standard Varian s2pul pulse sequence was used. The acquisition and delay times were respectively 0.8 and 0.5 s. Due to the poor abundance of ^{13}C nuclei, in order to obtain a good signal-to-noise ratio, 4000 scans were used. The spectra were analyzed for variations in chemical shift and line shapes using the software MNova.

2.3. Cloud point

The formulations for cloud point measurements were prepared by adding 6 % w/w C10E4 to water, together with a hydrophilic surfactant acting as a solubilizer. The solubilizer, selected from the options in Fig. 1, was added at concentrations aimed at maintaining most cloud point values between room temperature and 80 °C. The concentrations used were 6 % w/w for BC8Amph and LC12AO, 2 % w/w for LC12Amph, and 1.3 % w/w for LC12Quat. Systems were prepared with chelating agent concentrations ranging from 0 to 0.4 M. The pH was monitored and adjusted only if it deviated by more than one unit from the typical pH of MGDA or GLDA systems, which was approximately 9.5.

For the cloud point measurement, the formulation was added to a glass test tube containing a thermometer and heated in a water bath until complete turbidity was observed. The sample was then slowly cooled until a clear solution appeared. The temperature at which the system clarified was recorded as the cloud point. The process was repeated three times. To minimize practical difficulties and reduce error margins associated with measurements near the boiling point of water, cloud point measurements were capped at a maximum of 80 °C.

2.4. Surface tension

Surface tension measurements in binary systems were conducted using a surfactant concentration above its CMC, with varying concentrations of chelating agents (MGDA and GLDA) added to achieve surfactant-to-chelating-agent molar ratios of 2:1, 1:1, and 1:2.

The surface tension of the samples was measured using a du Noüy ring force tensiometer (Krüss K100). For each measurement, 50 mL of the sample was placed in a 70 mm diameter beaker. The ring circumference (R), provided by the manufacturer, was 9.545 mm. Surface tension was calculated by the tensiometer’s pre-programmed software based on the input parameters: ring dimensions, sample density, and a temperature of 25 °C.

2.5. Contact angle

Contact angle measurements for binary systems were conducted using the same formulations as those for surface tension measurements. For ternary systems, formulations from the cloud point measurements were used, selecting those with similar cloud point values and pH.

Contact angle measurements were conducted using an Attension Theta goniometer (Biolin Scientific AB). A 5 μL drop of the sample was placed on a parafilm surface, and an image of the drop was captured. The static contact angle at the three-phase boundary—where liquid, gas, and solid intersect—was determined by geometrically fitting the droplet contour.

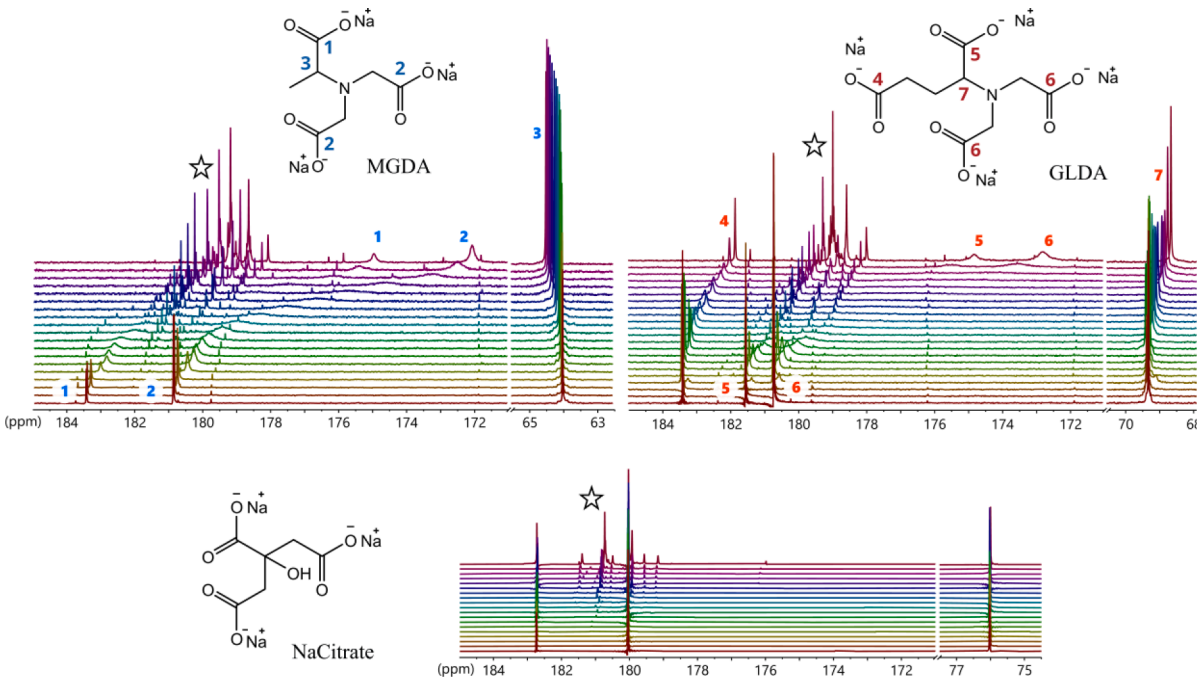

Fig. 2. Region of the ^{13}C NMR spectra evaluated for systems containing 0.24 M of chelating agents with increasing concentrations of LC12Amph. The chelating agents used were MGDA, GLDA and NaCitrate. The signal of a methylene group (around 70 ppm) was added as reference. Surfactant concentration increases progressively from bottom to top. Surfactant signals are marked with a star, while chelating agent signals are labeled with a number for consistent reference throughout the article.

3. Results and discussion

3.1. Structure of the chelating agent and its effect on the surfactant-chelating agent interaction

In this section, we investigate the effect of the structure of different chelating agents on their interactions with an amphoteric surfactant. By examining chemical shift changes and signal broadening in the ^{13}C NMR spectra, the nature and relative strength of these interactions was assessed. These insights contribute to a deeper understanding of how chelating agent structure affects their compatibility and efficacy in surfactant systems.

In systems containing MGDA and GLDA, Fig. 2 shows considerable chemical shift changes and signal broadening as the concentration of LC12Amph surfactant increases, affecting both the chelating agent and surfactant signals within this spectral region. This behavior indicates a progressive strengthening of the interactions with higher surfactant concentrations. Conversely, the system with NaCitrate as the chelating agent shows neither chemical shift changes nor signal broadening, suggesting the absence of interaction. These observations highlight the critical role of nitrogen in the chelating agent structure, as its presence appears essential for interaction with the surfactant under these conditions.

A more detailed examination of chemical shift and signal broadening in these systems is shown in Fig. 3, where both the chemical shift and signal width at half maximum amplitude are plotted as functions of the surfactant-to-chelating agent concentration ratio. It is important to note that in Fig. 2, the signals for C5 and C6 completely disappear by broadening at intermediate surfactant concentrations and reappear at higher surfactant concentrations. This prevents a detailed inspection of this region, leading to the observed gap in Fig. 3.

The comparison of the chemical shifts of MGDA and GLDA reveals a distinct variation for one carbon (C4 in GLDA) compared to the other carbons within the carboxylic groups of both chelating agents. Specifically, the chemical shift variation for C4 is 1.6 ppm, which is higher than that of non-interacting methylene groups, such as C3 and C7 (~0.7 ppm, see Fig. 2). However, this shift variation remains significantly smaller than that observed for the other carboxyl-bearing carbons (C1, C2, C5, and C6), which exhibit changes up to 10 times larger than those of the methylene groups. This suggests that while C4 is more affected than non-interacting methylene groups, it is far less affected than the other carboxylated carbons, indicating that the interaction at this position is less likely. The probable explanation is that the presence of additional carbon atoms between the nitrogen and the carboxylic group on C4 reduces its ability to engage in interactions with the surfactant—a trend also observed in the BC8Amph + GLDA system [12].

The following observations are more intricate and rely on the similarity of the carbon atoms of the carbonyl groups. Since these atoms are chemically alike, one would expect similar shifts if they would interact with the same molecule. Therefore, differences in chemical shift variations among these similar atoms provide useful insights into the probability of the interactions occurring.

For GLDA, one would expect similar changes in microenvironment for C5 and C6 due to interactions, and magnitude of observed chemical shift changes would be comparable. Focusing on the observed chemical shift of C5, it should be comparable whether the interaction occurs through C4 or C6, as the surrounding environment for C5 would remain similar regardless of which adjacent carboxylic group is involved in the interaction. The same rationale applies to the chemical shift of C6. However, our results show that the signal for C5 undergoes a smaller variation than that for C6, with a notable difference of around 1.2 ppm. This difference is significant, as it accounts for about 20 % of the total change of chemical shift experienced by these signals. A similar but smaller difference is evident between the signals for C1 and C2 in MGDA. The alpha carbons adjacent to both C1 and C5 have a branching, which likely introduces steric hindrance, reducing the probability of interaction with the surfactant. Notably, the branching on C1 is a methyl group, whereas C5 features a propionic acid group. The latter, being significantly larger, has a more pronounced effect on the chemical shift variation. Additionally, the methyl group contributes to binding affinity through its electron-donor nature, which likely competes with the steric effect, resulting in a smaller difference in chemical shift variation.

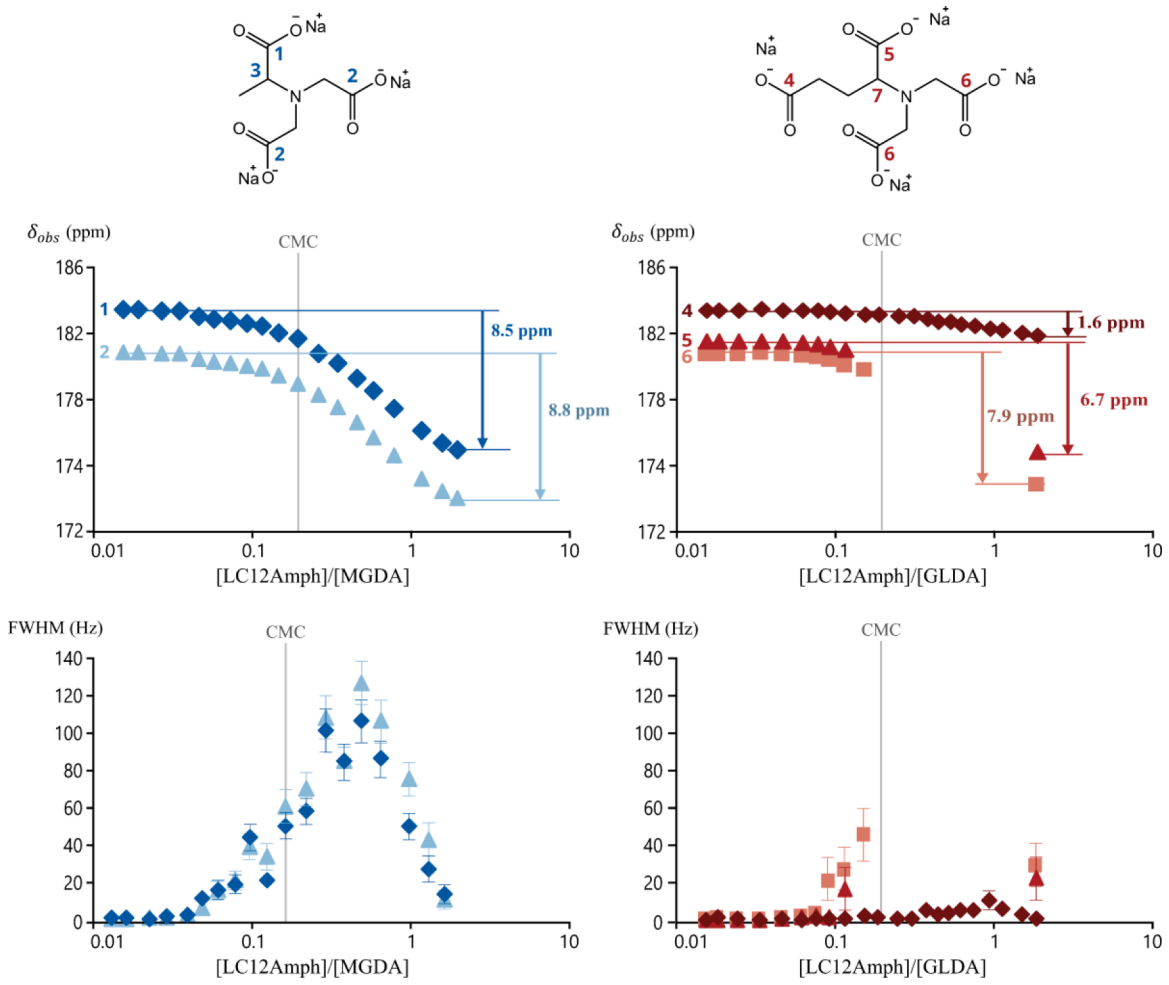

Fig. 3. Chemical shift (top) and signal width at half-maximum intensity (bottom) as a function of the surfactant-to-chelating agent concentration ratio for systems containing LC12Amph with MGDA (left panel) and GLDA (right panel). The tracked signals correspond to carbons within the carboxylic groups of each chelating agent, with numbering provided in the accompanying chemical structures. Error bars represent an estimated uncertainty of 10% of the measured signal width. Since the broadest signals were manually measured using image analysis tools, this estimate reflects a decreasing accuracy as the signal width increases. Note that the reported error bars are larger than the actual measurement error. The missing error bars are small and within the size of the markers used. Increasing surfactant concentration leads to notable shifts and signal broadening that provides insight into the distinct interaction behaviors of each chelating agent.

As can be seen in Fig. 3, MGDA signals generally exhibit larger chemical shifts variations as compared to GLDA. To explain these observations, we can turn to a theoretical framework based on the pseudophase transition model [13]. According to this model, the observed chemical shift of a resonance peak is a population-weighted average of interacting and non-interacting chelating agent molecules and can be expressed as:

$$\delta_{\text{obs}} = \delta_{\text{int}}\left(\frac{C_{\text{int}}}{C_{\text{T}}}\right) + \delta_{\text{not int}}\left(\frac{C_{\text{not int}}}{C_{\text{T}}}\right) \quad (1)$$

where δ_{int} and $\delta_{\text{not int}}$ represent the chemical shifts corresponding to the interacting and non-interacting forms of the chelating agent, respectively. The variables C_{int} and $C_{\text{not int}}$ denote the concentration of interacting and non-interacting chelating agent, respectively, and $C_{\text{T}} = C_{\text{int}} + C_{\text{not int}}$ represents the total concentration of chelating agent.

Note that for each carbonyl signal in the chelating agent molecule, the chemical shift for the interacting species, δ_{int}, reflects contributions from the various possible functional groups through which the molecule might interact with the surfactant. This can be written as

$$\delta_{\text{int}} = \sum_{i=1}^{n} \delta_{\text{int},C_i}\left(\frac{C_{\text{int},C_i}}{C_{\text{int}}}\right) \quad (2)$$

where n represents the number of chemically different available carbonyls that the chelating agent possesses for the interacting sites. For GLDA, n = 3, and for MGDA, n = 2.

Eq. (2) suggests that each carbonyl in the chelating agent can exhibit different chemical shifts based on its interaction state. If the chelating agent is not interacting with a surfactant, $\delta_{\text{obs}} = \delta_{\text{not int}}$. When a carbonyl is fully engaged in an interaction, its corresponding NMR signal will display a maximum change in chemical shift. If the interaction only involves another carboxylic group within the chelating agent, the observed chemical shift will fall between the non-interacting and the fully interacting values. As the probability of interaction for a particular carbonyl increases, the contribution of the interacting state becomes more dominant in the overall observed chemical shift for that specific carbon.

This occupancy distribution explains the smaller chemical shift variation of GLDA signals vs MGDA signals. With GLDA, there are four potential interaction sites, which suggests that each site has, on average, a lower probability of interacting with the surfactant compared to the MGDA which has only three available sites. This higher probability experienced by the individual carbon atoms of MGDA contributes to a more pronounced chemical shift variation.

To assess the strength, and not only the degree of occupancy, of interactions between the chelating agents and the surfactant, it is

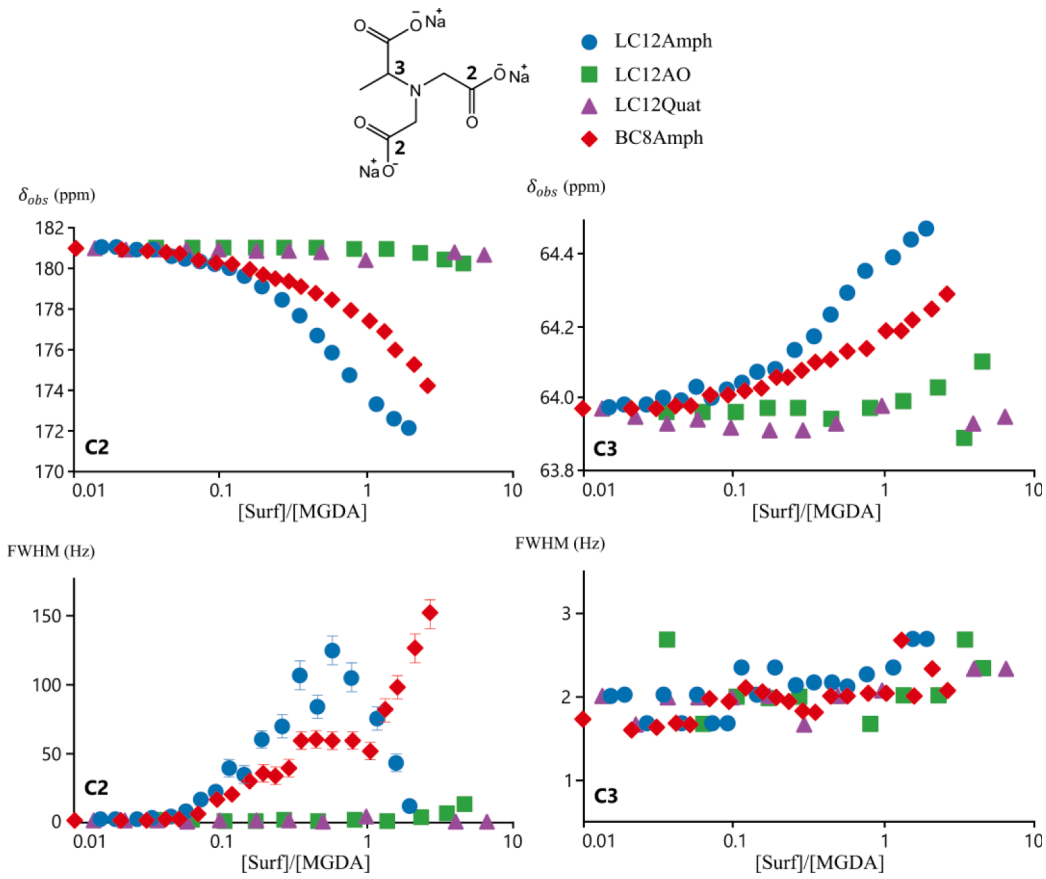

Fig. 4. Chemical shift (top) and signal width at half-maximum intensity (bottom) as a function of the surfactant-to-chelating agent concentration ratio for systems containing MGDA with four different surfactants: LC12Amph, LC12Quat, LC12AO, and BC8Amph. The tracked signals in MGDA correspond to a carbon within a carboxylic group (C2 in the left panel) and an alpha methylene carbon (C3 in the right panel), as indicated in the accompanying chemical structure. Note that the y-axis range for C3 is significantly smaller than that for C2, indicating that the observed changes in C2 are considerably larger than those for C3. Error bars represent an estimated uncertainty of 10% of the measured signal width. Since the broadest signals were manually measured using image analysis tools, this estimate reflects a decreasing accuracy as the signal width increases. Note that the reported error bars are larger than the actual measurement error. The missing error bars are small and within the size of the markers used.

necessary to examine changes in the broadening of the ^{13}C signal rather than the chemical shift. Signal broadening in NMR can have two origins: (i) decrease of T_2 spin relaxation and (ii) intermediate exchange rates between the extremes of fast or slow exchange. Since the adjacent carbons to the carbonyl groups (e.g. C3 and C7 in Fig. 2) do not exhibit broadening in the signal, the T_2 effect is minimal since translational spin relaxation is dominated by rotational correlation time. Thus, the observed changes in broadening upon higher surfactant concentration results from lower exchange rates, corresponding to longer residence times and stronger interactions.

For MGDA, the signal intensity due to broadening as a function of surfactant concentration reaches a minimum, after which the signals begin to sharpen. The initial broadening corresponds to an increase in interaction strength between MGDA and LC12Amph as the surfactant concentration increases, while the subsequent sharpening suggests a weakening of this interaction. We hypothesize that this effect is due to changes in micelle packing structure, where surfactant-surfactant interactions among the head groups compete against surfactant-chelating agent interactions displacing MGDA molecules.

GLDA signals also show a nonmonotonic broadening trend, with complete signal broadening down to spectral baseline in the intermediate concentration region. This behavior indicates a reduced molecular mobility and stronger surfactant-chelating agent interactions, compared to MGDA.

When comparing signal broadening for the same chelating agent, such as C5 vs. C6 and C1 vs. C2, the broadening is similar, suggesting comparable interaction strengths for these non-equivalent carbons. These findings indicate that steric hindrance from adjacent groups—such as those next to C1 and C5—does not significantly influence the interaction strength itself. However, as previously noted, such groups do affect the probability of interaction, likely by altering spatial accessibility. Finally, the minimal broadening of C4 across the concentration range suggests it interacts weakly with LC12Amph.

3.2. *Structure of the surfactant and its effect on the surfactant-chelating agent interaction*

In this section, the effect of the chemical structure of the surfactant on the interaction with the chelating agent was investigated. MGDA was selected for this evaluation due to its significant chemical shift response, which also remains clearly detectable across the full concentration range of surfactant tested (as seen in Fig. 2 and Fig. 3). By keeping the chelating agent constant and varying the surfactant structure, this analysis aims to reveal how different surfactant properties affect the strength and nature of interactions, offering further insight into the role of surfactant composition in modulating chelating agent behavior within these systems.

The comparison of amphoteric surfactants with amine oxide and quaternary ammonium-based surfactants reveals substantial differences in the chemical environment experienced by the chelating agent, as the surfactant concentration increases (Fig. 4). For the systems containing amphoteric surfactants, MGDA experiences significant changes in its

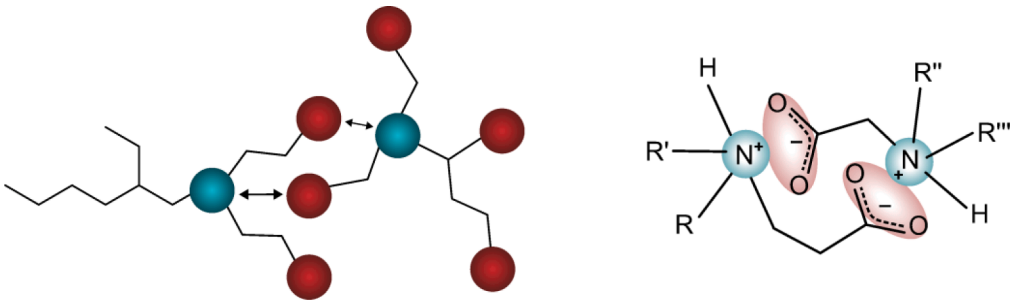

Fig. 5. Proposed interaction mechanism between an amphoteric surfactant and a chelating agent at pH values near their pKa values. The electrostatic interaction between the positively charged amine group and the negatively charged carboxylate groups is thought to drive the association.

chemical environment with increased concentration of surfactant, resulting in pronounced chemical shift changes for the signals. In contrast, LC12AO and LC12Quat cause only minor shifts, and these are apparent only when the surfactant-to-chelating agent ratio exceeds one, in the case of LC12Quat the change is even more subtle. The trends described here are consistent across all monitored carbons of MGDA, with considerably larger chemical shift variations observed with the carbons of the carboxylate groups (C2) compared to the methylene carbons (C3), as expected.

The changes in signal width are aligned with the observation for the chemical shift, with a significant broadening seen in systems containing amphoteric surfactants, and no changes in the presence of LC12AO and LC12Quat. These findings suggest that for effective interaction, not only is a positively charged surfactant required, but the surfactant must feature a head group with both positive and negative moieties. Moreover, the number of carbon atoms between these moieties appears to be crucial: it should neither be too short, as in the case of amine oxide, nor too long, as seen with the longest chain in GLDA. However, this is not the only difference between the head groups of LC12AO and LC12Amph, differences in electronic density may be influencing the surfactant-chelating agent interactions, with the harder, less delocalized density of amine oxides contrasting with the softer, more delocalized density of carboxylic groups.

Comparing amphoteric surfactants introduces additional complexity due to differences in their molecular structures, including variations in lipophilic chain length, branching, and the number of nitrogen-carboxylic pairs in the head group. Among these factors, the length and shape of the lipophilic chain likely play the most significant role in explaining the differences in signal broadening behavior. LC12Amph, with its long, linear chain, exhibits stronger self-association tendencies, leading to a non-monotonic change in signal broadening due to better micellar packing and competing head-to-head and head-to-chelating

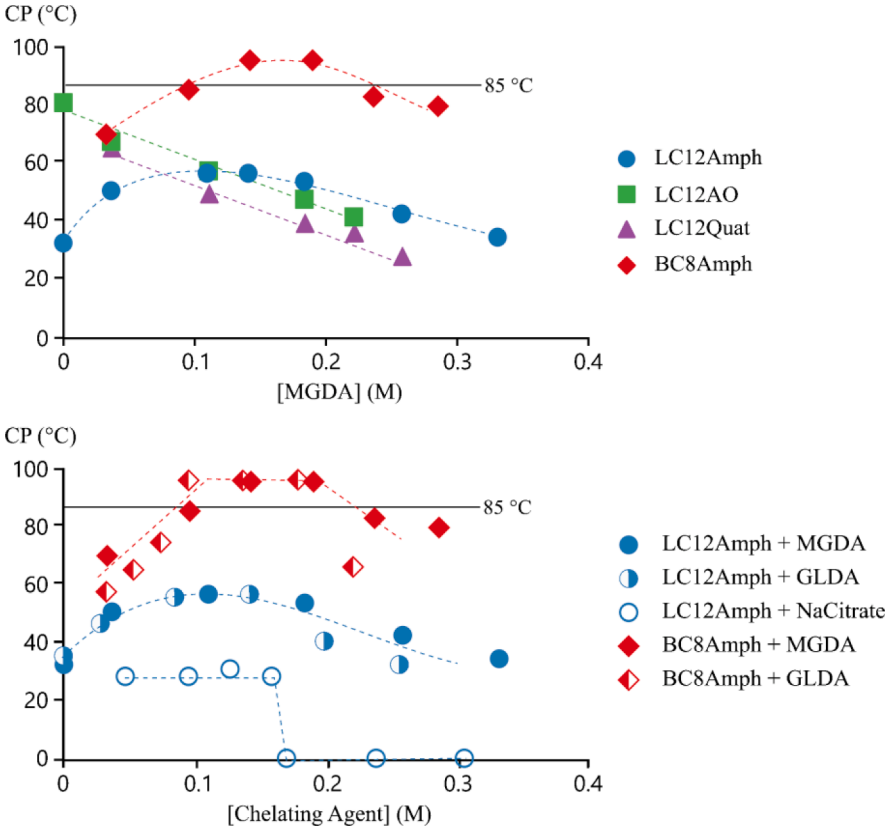

Fig. 6. Evolution of the cloud point as a function of chelating agent concentration. The formulations contained 6 % w/w C10E4 along with one solubilizer: 6 % w/w BC8Amph, 6 % w/w LC12AO, 2 % w/w LC12Amph, or 1.3 % w/w LC12Quat. Top: Cloud point changes for systems with various surfactants in the presence of MGDA. Bottom: Cloud point changes for systems with amphoteric surfactants and different chelating agents. Data above the 85 °C line is indicative only, as measurements were capped at 80 °C. The uncertainties of the measurements are small and within the size of the markers used. Dotted lines serve as visual aids.

agent interactions. In comparison, BC8Amph has limited self-assembly capacity, leading to poor packing and weaker head-to-head interactions, which in that context, makes it behave as a hydrotrope. As a result, the surfactant head groups are not close enough to interact effectively, leaving no significant competition against the surfactant-chelating agent interactions. This explains the monotonic increase in signal broadening as the concentration of BC8Amph increases in presence of chelating agent. Additional details on the competing interactions evaluated from the signal broadening of carboxylate groups on the amphoteric surfactants are provided in Fig. S1, Supporting Information. As the surfactant concentration increases, the signal broadening for the carboxylate groups in LC12Amph becomes more pronounced. In contrast, no significant change in signal broadening is observed for the carboxylate groups in BC8Amph.

The proposed interactions between amphoteric surfactants and chelating agents of the aminopolycarboxylic type in aqueous solutions are presented in Fig. 5. Given the pKa values of GLDA (9.5) and BC8Amph (10.2), and the fact that the experiments were conducted at pH values close to these pKa values, a significant fraction of both molecules have protonated nitrogen groups. At this pH, all carboxylic groups remain deprotonated. As a result, a fraction of molecules from both the surfactant and the chelating agent possesses both positively and negatively charged groups, separated by a distance of 2–3 carbon atoms.

The interaction between these molecules is thought to be driven by electrostatic forces between the positively charged amine group and the negatively charged carboxylate groups.

3.3. Effect of the interaction on the bulk properties

After demonstrating the existence of strong interactions between surfactants and chelating agents at the molecular level, it was essential to explore how these interactions may influence the bulk properties of potential cleaning formulations. One relevant property in water-based systems is the cloud point, which is a characteristic feature of polyoxyethylene-based surfactants. Therefore, the study includes an ethoxylated decyl alcohol with four ethoxyl groups (C10E4), a nonionic surfactant that is not water-soluble at room temperature. Its limited solubility allows for the measurement of the cloud point and offers insights into the practical implications of surfactant-chelating agent interactions.

Fig. 6 confirms our previous findings. When non-interacting species are used to solubilize the nonionic surfactant, increasing the concentration of the chelating agent results in a salting-out effect, lowering the cloud point of the system. This behavior was observed in systems containing either a water-soluble nonionic surfactant (decyl alcohol with eight ethoxylated groups) or sodium dodecyl sulfate as a solubilizer, using GLDA as the chelating agent [12]. A similar trend was observed here with LC12Quat and LC12AO using MGDA as the chelating agent, as well as in systems containing the LC12Amph-NaCitrate combination.

When the nonionic surfactant is solubilized by an amphoteric surfactant, such as BC8Amph or LC12Amph, the cloud point increases with the chelating agent concentration until it reaches a maximum. This behavior can be understood through the Critical Packing Parameter (CPP) model, which predicts the structure and properties of surfactant mixtures by accounting for surfactant geometry and environmental factors [14–16]. Specifically, the increased cloud point reflects a decrease in micellar size, likely due to an increase in the area occupied by the hydrophilic head group, attributed to complex formation between the chelating agent and the surfactant head group [12]. This shift reduces the CPP, which favors the formation of smaller, more spherical micelles.

The CPP itself incorporates variables such as the volume and length of the lipophilic chain and the area of the polar region, which depends on both the structure of the hydrophilic head group and its surrounding environment. The volume, V, and the length, l, of the lipophilic chain, based on the number of carbon atoms and branching, can be calculated using the formula

$$\frac{V}{l} = \frac{27(n_C + n_{Me})}{1.5 + 1.27n_C} \tag{3}$$

where n_C and n_{Me} represent the number of carbon atoms and methyl groups in the lipophilic chain, respectively.

The data in Fig. 6 supports the correlation between the interactions and changes in micellar size. For example, the cloud point shift for BC8Amph is significant, with a difference of at least 40 °C between the cloud points of systems at low chelating agent concentration and those at the maximum cloud point measured. In contrast, LC12Amph has a more moderate change of around 30 °C. In both cases the range of the cloud point values is independent of the chelating agent used.

The comparison of the volume-to-length ratios of the lipophilic chains for LC12Amph (21 Å^2) and BC8Amph (30 Å^2) further explains the observed differences in micellar size shifts. A similar change in the area of the hydrophilic head group leads to a larger shift in CPP for BC8Amph, resulting in a more substantial change in micellar size and, consequently, cloud point values compared to LC12Amph.

To facilitate a direct comparison between the ^{13}C NMR data presented in Fig. 4 and the cloud point data presented in Fig. 6, an additional plot has been included in the Supporting Information (Fig. S2). In this plot, the cloud point data is reported as a function of the surfactant-to-chelating agent concentration ratio.

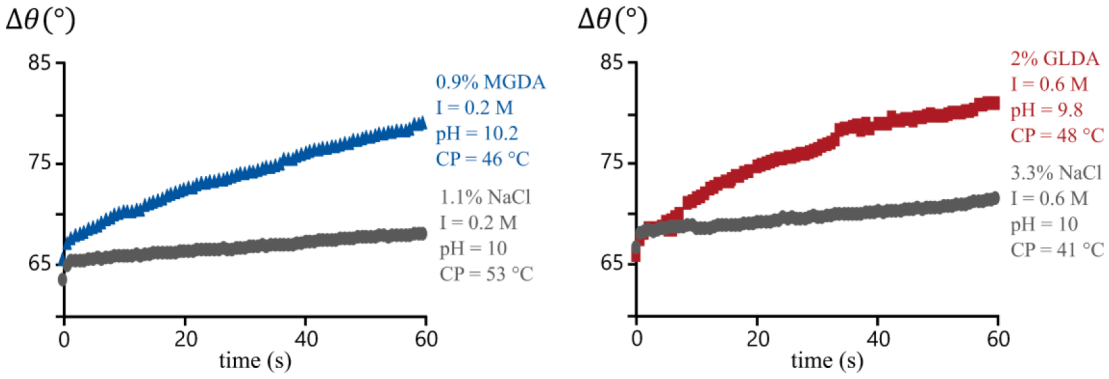

Fig. 7. Changes in contact angle (Δθ) relative to water for ternary systems containing LC12Amph, a nonionic surfactant (C10EO4), and either a chelating agent (MGDA on the left, GLDA on the right) or a salt (NaCl) with NaOH to match ionic strength, pH, and cloud point. The contact angle values are calculated by subtracting the contact angle of water from the measured contact angle of each formulation, therefore an increase in $\Delta\theta$ indicates enhanced wetting of the soiled surface. The uncertainties of the measurements are small and within the size of the markers used.

3.4. Effect of the interaction on the surface properties

While the interactions in surfactant-chelating agent and their consequences are demonstrated in bulk, it was equally important to understand how these interactions influence the surface properties of the formulations. This section examines changes in surface tension and contact angle in both binary systems of amphoteric surfactants with chelating agents and ternary systems incorporating nonionic surfactants. The ternary systems were selected to have comparable cloud points, ionic strength, and pH levels.

In the binary systems, no significant changes in surface tension or contact angle were observed, as shown Fig. S3 and Fig. S4, Supporting Information. The observed differences are primarily attributed to the intrinsic properties of the surfactants themselves. Systems containing more lipophilic surfactants, such as LC12AO, exhibit lower surface tension and contact angle values. In contrast, more hydrophilic surfactants, such as BC8Amph, display higher surface tension and contact angle values. These findings underscore that the addition of chelating agents does not significantly alter the surface-active properties of amphoteric surfactants in binary systems.

This is in agreement with expectations, as the interaction occurs primarily in the bulk, increasing the hydrophilicity of the surfactant. According to the rule of mixtures for surfactants, the less hydrophilic surfactant tends to populate the surface, meaning that the surfactant molecules interacting with the chelating agent has a reduced driving force to migrate to the surface.

In contrast to the behavior observed in binary systems, ternary systems exhibit distinct differences in contact angle measurements on surfaces soiled with hydrophobic materials, similar to those used to assess cleaning performance in industrial applications. The composition of the soil used is provided in the supporting information (SI 5). To account for variations in surface hydrophobicity, Fig. 7 reports the contact angle relative to that of water, calculated by subtracting the contact angle of water from the measured contact angle for each formulation. Consequently, an increased $\Delta\theta$ indicates enhanced wetting of the soiled surface. In systems containing LC12Amph with chelating agents, contact angle increased over time, showing a larger change than in systems adjusted to the same ionic strength, pH, and cloud point with NaCl and NaOH rather than chelating agents. This suggests that in ternary systems, the surfactant-chelating agent interaction may either promote the displacement of the less hydrophilic surfactant to the surface, or enable the mixed surfactant system at the soil/solution interface to draw more water molecules, thereby enhancing soil wetting.

4. Conclusion

To investigate the relationship between chemical structure and amphoteric surfactant-chelating agent interactions, we examined a series of amine-containing surfactants and polycarboxylic acid-type chelating agents. NMR spectroscopy served as a primary tool to monitor these interactions, while cloud point, surface tension, and contact angle measurements provided insights into the practical implications of the interactions.

Several key findings were reported regarding the interaction between chelating agents and amphoteric surfactants and their impact on formulation properties. It was found that oppositely charged moieties in both surfactants and chelating agents are essential to promote intermolecular interaction. The structure of these moieties plays a critical role: optimal spacing of one or two methylene groups between positive and negative charges enhances interaction probability and strength. Additionally, electron-donating groups and steric effects influence interaction probability, promoting or hindering interaction, respectively. While these effects were mainly observed for chelating agents, we hypothesize that they may also influence the surfactant head groups.

This interaction modifies micellar morphology by expanding the hydrophilic head group's area, a change most pronounced in surfactants with high volume-to-length ratios in their lipophilic chains. These structural features enhance both the strength of the interaction and its impact on formulation properties.

Finally, while binary systems showed minor effect on surface tension and contact angle, the introduction of a nonionic surfactant in ternary systems allowed these interactions to improve wetting behavior on hydrophobic surfaces. These findings suggest that the presence of a nonionic surfactant amplifies interfacial effects, a valuable insight for applications in which surface wetting and stabilization are critical.

Studies involving MGDA and GLDA are limited and tend to focus more on application-based research [9–11], often overlooking the molecular mechanisms that underpin these interactions. Our previous results [12] addressed this gap by experimentally evaluating the interactions between chelating agents like GLDA and an amphoteric surfactant. Building on the knowledge gained, here the structure–property relationships of surfactant-chelating agent systems were explored in greater depth advancing the understanding of the molecular interactions involved.

These findings highlight the importance of understanding surfactant-chelating agent interactions and their effects on surface properties, such as contact angle changes in ternary systems. Further investigation into the mechanisms underlying these effects would be valuable, particularly focusing on how molecular interactions between amphoteric surfactants, chelating agents, and nonionic surfactants influence the interfacial and surface properties of formulations. Clarifying their contributions to enhanced wetting and stability could provide strategies to fine-tune formulation properties, paving the way for improved surface-active systems across diverse applications.

CRediT authorship contribution statement

Josmary Velásquez: Writing – review & editing, Writing – original draft, Visualization, Investigation, Formal analysis, Conceptualization. **Sarah Lundgren:** Investigation. **Lars Evenäs:** Writing – review & editing, Supervision. **Romain Bordes:** Writing – review & editing, Supervision, Funding acquisition.

Declaration of competing interest

The authors declare that they have no known competing financial interests or personal relationships that could have appeared to influence the work reported in this paper.

Acknowledgements

This research work was financially supported by Nouryon Surface Chemistry AB and the Swedish Foundation for Strategic Research under Grant ID20-0039.

Appendix A. Supplementary data

Supplementary data to this article can be found online at https://doi.org/10.1016/j.jcis.2025.137606.

Data availability

No data was used for the research described in the article.

References

[1] Kołodyńska, D. Complexing Agents. in *Kirk-Othmer Encyclopedia of Chemical Technology* 1–26 (Wiley, 2019). doi:10.1002/0471238961.0308051208152301.a01.pub3.

[2] J.R. Hart, Ethylenediaminetetraacetic Acid and Related Chelating Agents, *Ullmann's Encyclopedia of Industrial Chemistry* (wiley (2011), https://doi.org/10.1002/14356007.a10_095.pub2.

[3] Y.U. Yangxin, J. Zhao, A.E. Bayly, *Development of Surfactants and Builders in Detergent Formulations*, *Chin. J. Chem. Eng.* 16 (2008).
[4] W. Zhao, et al., Aggregation of a Cationic Gemini Surfactant with a Chelating Molecule and Effects from Calcium Ions, *Langmuir* 33 (2017) 12719–12728.
[5] S. Soontravanich, H.E. Lopez, J.F. Scamehorn, D.A. Sabatini, D.R. Scheuing, Dissolution study of salt of long chain fatty acids (Soap Scum) in surfactant solutions, Part i: Equilibrium Dissolution. *J Surfactants Deterg* 13 (2010) 367–372.
[6] T.I. Yunusov, L.F. Davletshina, L.A. Magadova, M.A. Silin, Study of Chelating Agent-Surfactant Interactions on the Interphase as Possibly Useful for the Well Stimulation, *Energies (basel)* 16 (2023).
[7] I.S.S. Pinto, I.F.F. Neto, H.M.V.M. Soares, Biodegradable chelating agents for industrial, domestic, and agricultural applications—a review, *Environ. Sci. Pollut. Res.* 21 (2014) 11893–11906.
[8] Nowack, B. & VanBriesen, J. M. *Chelating Agents in the Environment*. https://pubs.acs.org/sharingguidelines (2023).
[9] X. Deng, et al., Wettability Alteration of Carbonate Rock by Chelating Agents and Viscoelastic Surfactants: Synergetic Impact, *Energy Fuel* 36 (2022) 7391–7401.
[10] Hassan, A. *et al.* Applications of chelating agents in the upstream oil and gas industry: A review. *Energy and Fuels* vol. 34 15593–15613 Preprint at https://doi.org/10.1021/acs.energyfuels.0c03279 (2020).
[11] H.Z. Hazrina, M.S. Noorashikin, S.Y. Beh, S.H. Loh, N.N.M. Zain, Formulation of chelating agent with surfactant in cloud point extraction of methylphenol in water, *R Soc Open Sci* 5 (2018).
[12] J. Velásquez, L. Evenäs, R. Bordes, The role of chelating agent in the self-assembly of amphoteric surfactants, *J Colloid Interface Sci* 676 (2024) 1079–1087.
[13] H. Wennerström, B. Lindman, Micelles, Physical Chemistry of Surfactant Association, *Physics Reports (review Section of Physics Letters)* 52 (1979) 1–86.
[14] B. Kronberg, K. Holmberg, B. Lindman, *Surface Chemistry of Surfactants and Polymers*, (wiley (2014), https://doi.org/10.1002/9781118695968.
[15] M.J. Rosen, J.T. Kunjappu, *Surfactants and Interfacial Phenomena*, (wiley (2012), https://doi.org/10.1002/9781118228920.
[16] D.F. Evans, H. Wennerstroem, *The Colloidal Domain Where Physics, Chemistry and Biology Meet.* (willey-VCH (1999).